River Flow 2010 - Dittrich, Koll, Aberle & Geisenhainer (eds) - © 2010 Bundesanstalt für Wasserbau ISBN 978-3-939230-00-7

Downstream-migrating antidunes in sand, gravel and sand-gravel mixtures

F. Núñez-González & J. P. Martín-Vide
Hydraulics Department, Technical University of Catalonia, Jordi Girona 1-3, D1, 08034 Barcelona, Spain

ABSTRACT: Downstream-migrating antidunes occur at upper-regime flows, but in contrast to the upstream-migrating antidunes, there have been a scarce number of reports about them in literature. Likewise, little is known about the characteristics of upper-regime and transitional bedforms when the bed sediment is not composed of a unique grain-size. In this study, flume experiments are described, for which mobile-bed equilibrium conditions were obtained for flows at, and close to, the transition between lower- and upper-regimes. High sediment feeding rates, even as high as 1 kg per second, were required for reproducing such conditions, for which three-dimensional downstream-migrating antidunes were the most frequent bedforms observed. Bed material for the experimental runs was composed of sand, gravel and two sand gravel mixtures, with average sand contents of 32% and 44%, respectively. A good agreement was found when comparing experimental results with bedform existence fields developed with potential flow theory, with the exception of the direction of movement of transitional bedforms, which theory failed to predict adequately. Mean flow velocity-wave length theoretical equations did not perform well for three-dimensional downstream-migrating antidunes, possibly because of the difficulties of defining adequately a transversal border condition.

Keywords: Bedforms, Upper-regime, Antidunes, Sand, Gravel, Sediment-mixtures

1 INTRODUCTION

Bedforms produced by water flowing over an alluvial bed have an important feedback effect on flow and are closely related to sediment transport. The understanding of them is, therefore, essential for the study of river hydraulics and sediment transport mechanics.

Bedforms developed in sand beds have been widely studied in experimental flumes and rivers. Bedforms composed of grain-size mixtures, however, have received less attention. In particular, few observations exist for transitional and upper-regime bedforms composed of mixed-size material.

In this study we report experimental bedforms in beds composed of sand, gravel and two sand-gravel mixtures, for flows with Froude numbers near to 1. The most frequent bedforms observed in the experiments were short-crested downstream-migrating antidunes; such bedforms are rarely reported in literature in comparison to the long-crested upstream-migrating antidunes and flat bed, with which upper-regime flow is normally associated.

The main distinctive characteristics of the bed features formed during the experiments are highlighted, and a comparison is presented with potential flow theory.

1.1 *Dunes and antidunes*

Dunes are the most characteristic bedforms in fully-rough turbulent subcritical flows (low Froude numbers). These forms migrate downstream and are asymmetrical in shape, with a gentle stoss-side slope and a steep slope on the leeside. The mechanism by which dunes move downstream is related to the flow separation eddy over the leeside, which induces deposition of material in front of the slip-face. On the other hand, bedforms typically associated with supercritical flows have been generally classed as antidunes, and the feature that most distinguishes them from dunes is the fact that the water surface undulations appear in-phase with the antidunes.

Bearing this defining attribute in mind, an attribute which involves the influence of the water surface standing-waves over the bed shape, antidunes are not only characteristic of supercritical flows, they are also likely to occur even under subcritical flow conditions.

Antidunes tend to be more symmetrical than dunes, showing a sinusoidal appearance, and move either upstream, downstream or remain stationary. As the direction of movement of antidunes is related to the sediment depositional pattern, distinctive relict internal sedimentary structures are associated with their migration direction. As such, some sedimentologists consider that the more generic term "in-phase waves" should be applied to upper-regime bedforms, so that downstream-migrating antidunes (DMA) and stationary antidunes should be distinguished from upstream-migrating antidunes (UMA) as different classes of bedforms in their own right (Cheel 2005).

Antidunes and dunes are classed as two-dimensional (2D) when their crest is straight transverse to the flow. Conversely, the shape of the so-called three-dimensional (3D) dunes and antidunes is more complex in plan form, and, in contrast to 2D forms, they often develop scour holes in their troughs. Given that the crests of 3D bed features are shorter than in 2D forms, 3D forms are also named short-crested. 3D bedforms occur for higher Froude numbers than their 2D counterparts. There is a scarce amount of literature available regarding reports on 3D antidunes.

1.2 *Bedform stability fields*

The ranges of flow conditions and sediment characteristics under which stable bedforms develop have been studied empirically by different authors, mostly for uniform sand-size material. Diagrams have thus been suggested with delimited stability fields for the occurrence of the different bedform classes (e.g., Vanoni 1974, Southard and Boguchwal 1990). Nevertheless, because of the lack of observations, some borders between bedform fields have been poorly defined or have been conceived of as intuitive extrapolations from the better-known regions. Furthermore, most stability fields specify *neither* a clear border between 2D and 3D bedforms, *nor* the conditions defining the direction of movement of antidunes.

In considering the validity of empirical diagrams developed from uniform sand material, Carling (1999) found that stability fields in such diagrams can be extended to grain-sizes pertaining to coarse gravel. Likewise, Kleinhans et al. (2002) concluded that these diagrams are also valid for supply-limited bedforms in sand-gravel if the plots are used with the bed-load material instead of with the bed material.

Bedform existence fields can be drawn in accordance with stability analysis based on potential flow theory, developed by Anderson (1953), Kennedy (1961) and Reynolds (1965). Potential flow analysis allows for discrimination between 2D and 3D antidunes. In the same manner, the theory outlines the border between UMA and DMA. Nevertheless, a clear delimitation between upper-stage plane bed and DMA is not specified by theory.

1.3 *Bedforms at and close to the transition between lower- and upper-regime*

For fine sediment, transition from lower-stage bedforms to antidunes is characterized by an upper-stage plane bed region. It has been observed that for coarser grain-sizes such a plane bed might not occur, in such a way that the dunes phase can be followed by antidunes.

Carling and Shvidchenko (2002) compiled experimental and field-data belonging to bedforms in the dune-antidune transition in fine gravel and compared them with theory. Descriptions of transitional bedforms reported by different authors showed a variety of morphologies and characteristics that resemble those of dunes or antidunes, or both. Carling and Shvidchenko also contrasted data for DMA with potential flow theory and found an acceptable agreement. They also highlighted the need for more empirical data to delineate the dune-antidune phase transformation in gravel.

Little information exists about bedforms at, and close to, the transition between the lower- and upper flow regimes for sediment mixtures. In this sense, it is worth mentioning the work of Chiew (1991), who studied the effect of sediment gradation on the transition between bedform types. While he found no important effects, he did find a tendency towards the absence of antidunes for higher grain-size standard deviations, which he attributed to the formation of a dynamic armored layer.

In this study we present experimental observations of bed features formed in sand, gravel and two mixtures of these materials for flows with Froude numbers near 1. High-sediment transport rates were required, as the objective was to study bed features that get formed when all the bed material size-fractions are in motion. In a similar fashion to the previous studies described above, data are compared with potential flow theory, and possible reasons for deviations

between theory and experimental evidence are discussed.

2 BEDFORM STABILITY FIELDS OBTAINED FROM POTENTIAL FLOW THEORY

Following the original stability analysis outlined by Anderson (1953) and extended by Kennedy (1961), Kennedy (1963) presented relations for defining bedform stability fields as a function of the Froude number

$$Fr = \frac{V}{\sqrt{gH}} \tag{1}$$

and the wave number $k=2H\pi/L$, where g = gravitational acceleration, H = mean flow depth, L = length of the sediment wave, and V = mean flow velocity. In this manner, the upper-regime occurs when $Fr > Fr_u$, where:

$$Fr_u = \sqrt{\frac{\tanh(k)}{k}} \tag{2}$$

UMA are likely to occur for the range $Fr_u < Fr < Fr_p$, with Fr_p defined by:

$$Fr_p = \sqrt{\frac{1}{k\tanh(k)}} \tag{3}$$

The theory also allows for delimitation between 2D and 3D antidunes, such a border being given by:

$$Fr_d = \sqrt{\frac{1}{k}} \tag{4}$$

Equations 2, 3 and 4 are plotted in Figure 4.

DMA are likely to occur for large wave numbers if $Fr > Fr_p$ and $Fr > Fr_u$. In such a regime the water- and bed- surfaces are in-phase, but in contrast with UMA, the water-depth is greater over the troughs than over the crests, in a similar way to dunes, so that net sediment deposition occurs over the troughs (Carling and Shvidchenko, 2002; Parker, 2004).

Upper-stage plane bed for high Froude numbers cannot be predicted by theory. Nevertheless, for $Fr > Fr_u$ and low wave numbers ($k\rightarrow 0$), i.e., large wave-lengths, antidunes are depressed and upper-stage plane bed is likely to occur (Carling and Shvidchenko, 2002).

According to potential flow theory analysis, the wave-length of antidunes is related to the mean flow velocity by:

$$V = \sqrt{\frac{gL}{2\pi}} \tag{5}$$

This relation does not hold for 3D waves, which are shorter. Such waves on the water surface are formed by the coincidence of stationary waves in the flow direction and cross-waves transversal to the flow; these waves are also known as "rooster-tails". According to Hasegawa and Kanbayashi (1996, after Yokokawa, et al. 2008), short-crested antidunes are formed when the wave-lengths of 2D antidunes and water-surface diagonal-cross waves are the same. From a previous development by Fuchs (1952, in Kennedy, 1961), Kennedy presented the following functional relation between the mean flow velocity and the wave-length of 3D waves in which he considered that the waves celerity and the flow velocity are the same

$$V = \sqrt{\frac{gL}{2\pi}}\sqrt[4]{1+\left(L/L_t\right)^2} \tag{6}$$

where L_t = wave-length normal to the direction of flow, which as a first approximation can be taken as the channel width.

When contrasting equations (5) and (6) with experimental data in sand, Kennedy (1961) found a sound correlation between 2D waves, whereas he found an overestimation trend of the flow velocity for 3D antidunes. Kennedy estimated that the discrepancies for 3D waves could be due to considering the transverse wave-length of the rooster-tails as being equal to the channel width.

3 EXPERIMENTS PERFORMED

The objective of the experiments was to study the flow, sediment transport, and bed features developed at, and close to, the transition between lower- and upper-flow regimes. As a result, high sediment transport rates and flow discharges were required. In order to meet these requirements, a new experimental set-up was used, which was conceived so as to enable the performance of long-lasting runs with a constant feeding of mixed-size material, without requiring a large stock of sediment. This condition was achieved with a system that not only recirculated the sediment collected at the end of the channel, but also separated sand- and gravel-fractions, and fed each size-fraction back into the channel at a constant rate using an automatic feeder. A more detailed description of the feeding and recirculating systems can be found in Núñez-González and Martín-Vide (2009).

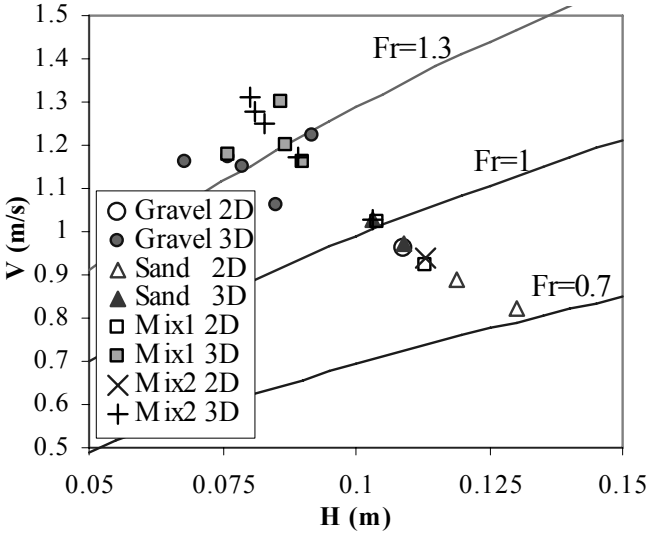

Figure 1. Range of experimental data. 2D and 3D refer to the dominant stationary-wave observed.

Four experimental series were performed, each for a different grain-size material, namely gravel, sand and two sand-gravel mixtures. Geometric mean diameters for the sand and gravel were 1.5 and 3.5 mm, respectively, and geometric standard deviations were 1.3 for the sand and 1.4 for the gravel. The sediment mixtures were obtained by mixing the original sand and gravel with an average proportion of 32% sand content for mixture 1 (Mix1) and 44% for mixture 2 (Mix2). Mix1 was slightly bimodal, while Mix2 was unimodal. Each experimental series consisted of 6 runs, except for the sand series, for which 4 runs were performed.

The experimental flume was rectangular, 30m long (27m effective length), 0.75m wide and 0.60m deep. Water-discharge was controlled with an automatic electronic flow-meter and was fed and recirculated independently from the sediment circuit. Water-depth, and bed- and water-slopes were obtained from measurements of the bed- and water-surface level performed at the channel's glass-paneled walls with rulers that were spaced one meter apart.

Experiments consisted in obtaining mobile-bed equilibrium conditions for a given water-discharge and sediment-feeding rate, mostly by erosion of the original bed profile, i.e., imposing higher flows than those required to transport the sediment fed into the channel. Prescribed unit water discharges and sediment-feeding rates ranged from 78 to 112 l/s/m and 0.081 to 1.07kg/s, respectively. The proof of mobile-bed equilibrium having been attained was the equality of the feeding- and the recirculated-sediment rates, and the persistence of average water-depths, bed- and water-slopes, and bedform dimensions over several hours.

During the equilibrium phase of the experimental runs the bedforms near the channel walls and the water-surface waves were observed, photographed and recorded in video. Some point measurements of some characteristics of the bed and water-surface waves were carried out as well, namely, celerity, amplitude and wave-length. In addition, bedload samples were taken at the downstream end of the channel using a sampler as wide as the channel. The sampler was divided into three parts of equal length, with the aim of proving possible transversal grain-size sorting trends.

At the end of each run, the bed surface was photographed, and surface- and subsurface-bed material samples were taken at different locations along the channel. Bed scour was measured at a section 4.5 meters upstream from the end of the channel by opening a vertical section where original bed-material had previously been replaced by gravel painted with different colors and set at 1cm thick successive horizontal layers.

4 EXPERIMENTAL RESULTS

The range of mean flow velocities, water-depths and Froude numbers measured during the equilibrium phase of the experimental runs is shown in Fig. 1. Equilibrium energy slopes ranged from 0.006 to 0.021, while bed shear stresses, after making modifications which took side-wall effects into account following the Vanoni and Brooks method, ranged from 5.8 to 16.3 Pa. Descriptions of the water- and bed-configurations, scour patterns and grain-sorting are presented as follows.

4.1 *Water surface configuration*

Trains of rooster-tails were observed during most of the runs (see Fig. 2), with varying characteristics of shape, geometry and stability. All the rooster-tails and water waves that were observed showed a net downstream displacement, though a single wave could sometimes, for short periods, remain stationary, migrate upstream or disappear to rebuild again. For most of the runs the rooster-tails were stable in the sense that if they broke they reformed rapidly, while the train of rooster-tails was not markedly affected.

2D waves formed at the upper-part of the channel, some meters downstream from the sediment input, and they then transformed into rooster-tails, normally between 10 to 15 meters downstream from the sediment-input section. For a varying length of 3 to 6 meters the 3D waves kept growing in height and length until they

stabilized at a more or less fixed geometry, which was conserved until the end of the channel downstream.

The criterion for distinguishing between 2D and 3D waves, as plotted in Fig. 1, was mainly related to the dominant wave observed on the surface. Given that most of the runs showed rooster-tails, the criteria used to classify the water-surface as 2D was that the rooster-tail protruded slightly above the surface compared to the other stationary waves – if, that is, such waves were present – or compared to the sediment waves on the bed surface.

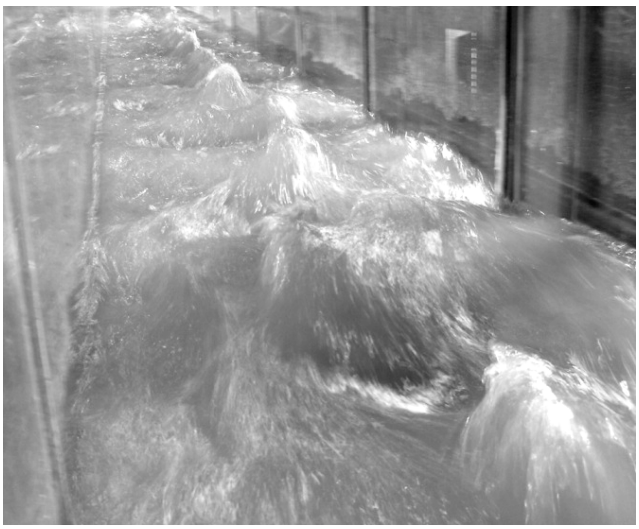

Figure 2. Train of short-crested stationary waves, "rooster-tails", for a sand-gravel sediment mixture with 32% sand content. Run with Fr=1.23. Mean wave-length is 62 cm. Flow from background to foreground.

4.2 *Bed configuration*

Above all in the case of the sediment mixtures run series, bed states observed during the runs consisted of the coexistence of two types of bedforms. On one hand, low amplitude features prevailed next to the channel walls. On the other hand, at the center of the channel 3D-DMA occurred under the rooster-tails. For sand- and gravel-runs, low amplitude bedforms might have been present as well, but could have remained hidden to direct observation because of the higher amplitude and lower wave-length of the dominant bedforms.

As with the rooster-tails, bed features observed next to the flume walls always migrated downstream and evolved along the channel until they reached a stable configuration. Usually, they were first noticeable 3 to 5 meters downstream from the upper-sediment input. From here to where they reached stability – i.e., 10 to 15 meters downstream from the sediment-input section – the features moved faster, and were shorter and lower than their stable counterparts at the last section of the flume downstream. Though we may refer here to a "stable" configuration, this should be considered within a statistical sense, given that for some runs the bedforms near the wall varied their shape and geometry continuously.

The shape of the bedforms near the channel walls and their degree of coupling with the water surface varied with the Froude number and the bed-material. For some conditions, such variation was important even within a single run. In general, unequivocal antidunes (i.e., bedforms which were an in-phase image of the water surface irrespective of their symmetrical or asymmetrical shape, see Fig. 3) appeared with higher Froude numbers for the gravel and mixtures than they did for the sand-run series. A similar trend was observed for transitional bed-states, which are here considered to be those characterized by, firstly, bedforms with a certain degree of coupling between water- and bed-surface and, secondly, those for which the bed configuration alternated between showing dunes and antidunes. Transitional bedforms observed consisted of downstream migrating features, mainly low-relief waves for the mixtures and gravel, and transitional dunes for the sand. Transitional bedforms were rounder the stronger the coupling with the water surface, and the higher the flow Froude number, were. Also, a separation eddy on their leeside was more evident for low Froude numbers, for which the features appeared sharp-crested.

Normally, on account of the turbidity of the water and the local unsteadiness of flow, it was not possible to observe the bedforms at the channel central section. Nevertheless, based on the scarce observations available we can assume that if and when rooster-tails occurred on the surface, then beneath these rooster-tails the bedforms were in-phase with the water wave, and thus can be classed as antidunes. What is more uncertain is the shape and size of these forms. Nonetheless, based on the isolated observations that it was possible to make, and in agreement with observations already made by Kennedy (1961) regarding sand beds, we can infer that the bed under the rooster-tails had the same 3D form as the surface waves, with the difference that the bed waves were neither as high nor as sharp as the surface waves.

Normally, when the water discharge was drawn down at the end of each run (this usually took between 1 and 2 minutes), most of the bedforms were erased. This type of behavior is typical of antidune configurations and is one of the main reasons why antidunes are so rarely preserved (Carling and Breakspear, 2007).

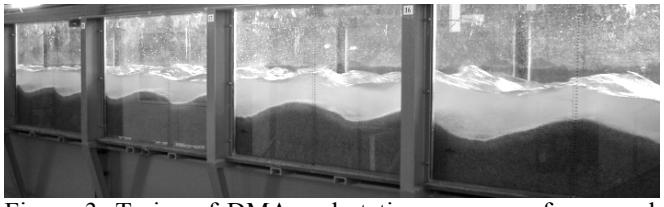

Figure 3. Trains of DMA and stationary waves for a sand run with Fr=1.02. Note that water and bed surfaces appear roughly in-phase, and that water-depth over the troughs is higher than over the crests. Mean wave-length is 53 cm. Flow from left to right. Length of glass panels is 1 meter.

4.3 *Bed scour patterns*

Though antidunes and other steep bedforms were washed away when the water discharge was stopped at the end of the run, the transversal profile of maximum scour that they produced was measured for the sand- and mixtures-run series by identifying the buried colored gravel that remained. For the mixtures, the deepest scour occurred at the center of the channel, except for the runs with the lowest Froude number. A direct qualitative relation was found between the observed strength of the rooster-tail during the run and the depth of scour at the central section. Conversely, scour profiles for the sand-runs were approximately uniform, i.e., the depth of scour was roughly the same all along the transversal section. Such a pattern reflects the tendency for the bedforms in the sand runs to be more two-dimensional than the runs with sediment mixtures, which showed a marked three-dimensionality for most of the runs.

4.4 *Differences between bed materials*

Overall, differences between bedforms for the four bed materials were less important for the gravel compared to the mixtures than they were for the sand compared with gravel and mixtures. For example, similar to the findings made by Kuhnle (1993) with regards to lower-regime bedforms in sand, gravel, and sand-gravel mixtures, we found that bedform amplitudes were higher the higher the sand content in the mixture was. In this manner, amplitudes of sand bedforms were 3 to 5 times higher than in mixtures and in gravel.

With respect to the sediment grain-size sorting for the mixtures-runs, a slight bias towards a finer bed-surface was noticed with increasing Froude numbers. On the other hand, bedload samples showed a subtle trend for coarser material to travel preferentially at the center of the channel. This tendency concurred with visual inspection of the sections opened to measure scour depths in the sense that open-framework gravels were often noticed at the central section.

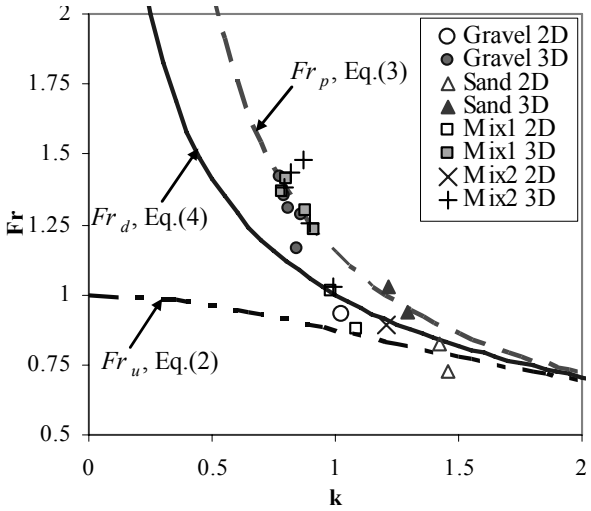

Figure 4. Comparison between experimental data for sand, gravel and sand-gravel mixtures, and bedform occurrence fields delimited with the potential flow theory.

4.5 *Comparison with potential flow theory*

Figs. 4 and 5 show plots of the experimental results compared with potential flow theory as outlined by Eqs. (1) to (6). As can be seen in Fig. 4, most of the data for 3D waves appear close to the curve used to, theoretically, delineate the upper limit for 3D antidunes as well as the lower limit for DMA (Eq. 3). As a result, we may say that theory corresponded adequately to observations for 3D-DMA, except for one gravel data-point and one mix1 data-point, which unequivocally appear inside the region for UMA. The same occurs for most of the rest of the data-points corresponding to 2D waves. For all of these runs the waves moved downstream, so that even when theory accurately predicts the bidimensionality of the majority, it fails to define the direction of their movement correctly.

Fig. 5 depicts the relation between mean flow velocity and wave-length as given by Eqs. (5) and (6), and shows the experimental data for comparison. For most of the 3D waves, Eq.(6) underestimates the experimental mean flow velocities. Conversely, Eq.(5) overestimates flow velocities for most of the 2D waves.

Experimental wave-lengths used for drawing Figs. 4 and 5 were obtained from measurements of rooster-tails and performed by two different methods. The first consisted in a direct measurement of the distance between crests of different waves during the runs using a tape-measure. For the second method the number of crests over a known distance was counted using photos of the last 10 meters of the channel. Standard deviations of the measurements were, on average, 10% of the mean wave-lengths. The procedures for obtaining an average wave-length were not *absolutely* accurate; firstly, because not many waves could be counted owing to the

limited length (10m) of the section observed, which, in turn, limited the number of measurements that could be made of the distance between the wave-crests, and, finally, because the distance between these crests varied significantly from one moment to another.

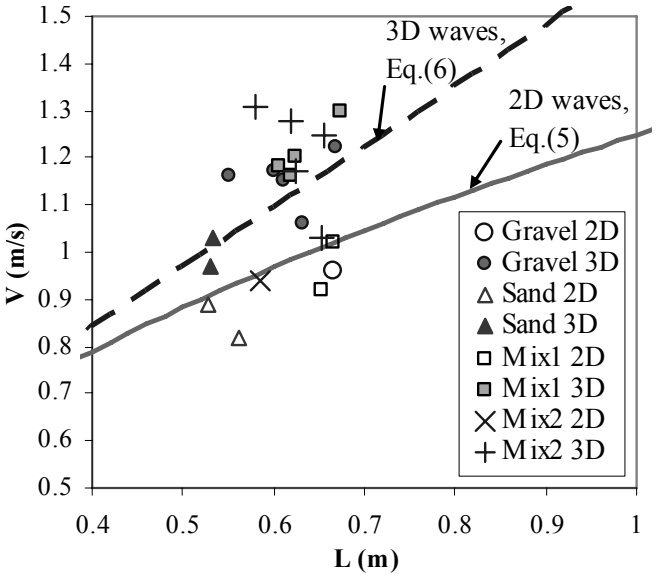

Figure 5. Comparison of measured flow velocities and wave-lengths with potential flow theory, Eqs. (5) and (6), for 2D and 3D waves, respectively.

5 DISSCUSSION

Wave-lengths used for plotting Figs. 4 and 5 were obtained from measurements of the rooster-tails observed in all of the experimental runs. However, based on the experimental observations it was clear that for some runs the dominant bed- and water-configurations were not necessarily 3D, although the water surface did show short-crested 3D waves. For this reason, these bed states were classed as 2D. On the other hand, if the dominant bed- and water-configurations were 2D, then it would follow that short-crested waves may not be necessarily linked to the bulk flow properties. Conversely, local-flow properties at the central section of the channel would be related to the formation of the rooster-tails, as opposed to the mean flow conditions. This would signify that an inconsistency exists in using the measured wave-lengths of the rooster-tails, which are a 3D feature, when applying potential flow theory to a predominantly 2D flow.

As a consequence, for flows with dominant 2D bed- and water-configurations, a different flow velocity than the section mean value should be used in order to coherently test the rooster-tails' existence with potential theory. Such a flow velocity would have to represent the conditions at the channel central section where the rooster-tails were formed. By proceeding in the reverse order, if we consider that Eq.(3) represents the stability conditions for 3D-DMA, we can obtain the flow velocities representative of the central section where the short-crested waves occurred. This is achieved by making Eqs.(1) and (3) equal, and using the measured k and H values. For all points originally indicated as 2D as well as for the two 3D outliers, such velocities were computed. Then, flow velocities obtained in this manner were used with Eq.(6) to compute theoretical wave-lengths. These 3D wave-lengths were found to have, on average, a difference of less than 3% when they were compared with the measured values; that is to say, this percentage is of the same order of magnitude as the measurement accuracy. This proves the appropriateness of relating the formation of short-crested waves in a predominantly 2D bed- and water-configuration to local flow conditions, rather than relating it to the section's average flow properties.

The preceding analysis reflects the transitional nature of flow between well established lower-regimes and upper-regimes. It also reflects the failure of potential flow theory to describe the bedform characteristics when applying the bulk flow properties in such a transition. As a consequence, the definition of the limits where the dune-antidune transition occurs is relevant. Carling and Shvidchenko (2002) considered that, due to lag-effects and possible depth-limitations, the range of Froude numbers within which transitional bedforms can persist in fine gravel varies between 0.5 and 1.8. Nevertheless, they found that, for most of the reported studies, transitional bedforms cannot occur for Fr > 1.3. Our results concur with this upper limit in light of the fact that the highest Foude number for the range of transitional bedforms observed was 1.3.

5.1 *Wave-length and occurrence of 3D-DMA*

In Fig. 4, most 3D-DMA plot within the region where potential flow theory predicts their existence. Nevertheless, wave-lengths in Fig. 5 are overestimated. One cause for this discrepancy is related to the transversal length of the short-crested waves since this length might not necessarily be equal to the channel width.

Although rooster-tails are formed by surface diagonal waves, channel-walls might not be a defining factor for their existence. Kennedy (1961) evidenced this assertion by quoting an experimental run performed at the Colorado State University, for which an isolated train of rooster-tails formed at the center of a 2.4m wide channel. For this run it was apparent that the vertical channel walls did not exercise any influence on the formation of the short-crested waves. As such,

the channel width might not necessarily be equal to the rooster-tail wave-length normal to the direction of flow used in Eq.(6). It is possible that the excavated scour-holes by the rooster-tails could, in some cases, set a transversal boundary narrower than the channel width.

The minimum wave-number for which DMA were reported in data collected by Carling and Shvidchenko (2002) was $k \approx 0.6$ (obtained from Fig. 8 in Carling and Shvidchenko, 2002). As shown in Fig. 4, the minimum wave number registered for DMA in the experimental runs of this study was $k=0.78$, which concurs with the former value.

6 CONCLUSIONS

Transitional bedforms and three-dimensional downstream-migrating antidunes were the most frequent bedforms observed in experiments performed in very coarse sand, very fine gravel and two sand-gravel mixtures, with flow conditions at, and close to, the transition between lower- and upper-regimes. Bedform stability-fields drawn after potential flow theory performed well when compared with the experimental observations, except for the transitional bedforms for which the direction of movement cannot be predicted. Functions relating flow velocity with wave-length failed to adequately describe the experimental results. For three-dimensional downstream-migrating antidunes such a disparity can be attributed to the difficulty of defining a proper transversal border condition.

ACKNOWLEDGMENTS

The first author was supported by the Programme Alβan, the European Union Programme of High Level Scholarships for Latin-America, No.(E04D048796MX), and by Conacyt, México (179047). The authors thank Professor Gary Parker for providing them with a digital copy of Kennedy's original study on antidunes.

REFERENCES

Anderson, A.G. 1953. The characteristics of sediment waves formed by flow in open channels. Third Midwest Conference on Fluid Mechanics, University of Minnesota, Minneapolis, Minn.

Carling, P.A., Breakspear, R.M.D. 2007. Gravel dunes and antidunes in fluvial systems. In Dohmen-Janssen, C.m. & Hulscher, S.J.M.H. (eds.), River, Coastal and Estuarine Morphodynamics: RCEM2007, Taylor & Francis: 1015-1020.

Carling, P.A., Shvidchenko, A.B. 2002. A consideration of the dune:antidune transition in fine gravel. Sedimentology, 49, 1269-1282

Carling, P.A. 1999. Subaqueous gravel dunes. J. of Sedimentary Research, 69(3), 534-545

Cheel, R.J. 2005. Introduction to clastic sedimentology. Course Notes. Department of Earth Sciences, Brock University, Ontario, Canada

Chiew, Y.M. 1991. Bed features in nonuniform sediments. J. of Hydraulic Engineering, 117(1), 116-120

Fuchs, R.A. 1952. On the theory of short-crested oscillatory waves. Gravity Waves, National Bureau of Standards Circular 521, 187-200

Hasegawa, K., Kanbayashi, S. 1996. Formation mechanism of step-pool systems in steep rivers and guide lines for the design of construction. J. of Hydroscience and Hydraulic Engineering 40, 893-900. (in Japanese with English abstract)

Kennedy, J.F. 1963. The mechanics of dunes and antidunes in erodible bed channels, J. of Fluid Mechanics, 16, 521-544.

Kennedy, J.F. 1961. Stationary waves and antidunes in alluvial channels. Rep. no. KH-R-2. W.M. Keck Laboratory of Hydraulics and Water Resources, California Institute of Technology, Pasadena, CA, 146 pp.

Kleinhans, M.G., Wilbers, A.W.E., De Swaaf, A., Van Den Berg, J.H. 2002. Sediment supply-limited bedforms in sand-gravel bed rivers. J. of Sedimentary Research, 72(5), 629-640

Kuhnle, R.A. 1993. Fluvial transport of sand and gravel mixtures with bimodal size distributions. Sedimentary Geology, 85, 17-24

Núñez-González, F., Martín-Vide, J.P. 2009. Bed resistance and sediment transport experiments in sand, gravel and sand-gravel antidunes. 33th IAHR Congress, Water Eng. for a Sustainable Environment, Vancouver, Canada

Parker, G. 2004. 1D Sediment transport morphodynamics with applications to rivers and turbidity currents. Chap. 8. Fluvial Bedforms. E-Book: http://cee.uiuc.edu/people/parkerg/morphodynamics_ebook.htm

Reynolds, A.J. 1965. Waves on the erodible bed of an open channel. J. of Fluid Mechanics, 2*2*, 113-133

Southard, J.B., Boguchwal, L.A. 1990. Bed configuration in steady unidirectional water flows; Part 2, Synthesis of flume data. J. of Sedimentary Petrology, 60(5), 658-679

Vanoni, V. 1974. Factors determining bed forms of alluvial streams. J. of Hydraulic Engineering, 100(3), 363-367

Yokokawa, M., Hasegawa, K., Kanbayashi, S., Endo, N. 2008. 3D antidunes preserved on fine-grained sand bed in an experimental flume: Genetic conditions and their sedimentary structures. Marine and River Dune Dynamics. Leeds, U.K., 345-351